ISSN 2522-9400 **European Modern Studies Journal** *Vol 8 No 5*
available at www.journal-ems.com
DOI: 10.59573/emsj.8(5).2024.30

Dynamics and Bifurcation in Fibre Fuse Phenomenon

Ervis Gega [1] *, Dode Prenga [2]
[1] Department of Radiation Protection and Monitoring Network,
Institute of Applied Nuclear Physics, University of Tirana, Albania
[2] Department of Physic, Faculty of Natural Science, University of Tirana, Albania

Abstract. In many physical systems, we encounter periodic behaviours otherwise called oscillations. Their nonlinear dynamics show us spirals, limit cycles, sudden Hopf jumps, and chaotic behaviour. An important case of oscillations is the relaxation oscillation well represented by the self-contained oscillator Van der Pol which exhibits a Hopf bifurcation after crossing a threshold. Such an oscillation pattern is encountered in the oscillation of plasma charge density. Solving Maxwell equations and modelling magnetohydrodynamics equations for such a plasma, where a nonlinear source term will prevail which will bring about a negative friction, will determine a relaxation oscillation under specific conditions and quasi-chaotic behaviour for certain cases. These oscillations appear in dusty interstellar plasmas and the optical fibre fuse. A qualitative method for understanding the dynamics of this system is the use of nonlinear dynamic methods, but to get an exact solution we need to integrate the system numerically. Numerical integration of plasma oscillations gives us clear numerical values needed to consider engineering applications.

Key words: Oscillation, Hopf bifurcation, Numerical integration

Introduction

The model of oscillatory processes has an irreplaceable role in physics. Nonlinear oscillators present a wide variety of behaviours starting from simple damped oscillations continuing with relaxation oscillations to chaotic oscillations in the case of coupled oscillators (Strogatz, 2003). Studying these models in the context of nonlinear dynamics highlights additional elements of stability and instability, including Hopf jumps of solutions when a parameter exceeds a certain target. For the exact solution of the performance of the systems, numerical techniques are necessary mainly for engineering-application purposes.

A specific case of oscillations is those modelled with the Van der Pol system (Pol, 1926). In an approximate way, these behaviours are found in physical, biological, engineering, economic, etc. systems (Miwadinou et al., 2013; Semenov et al., 2006). They are well-studied ranging from heartbeats and relaxing oscillations of potential in neuronal cells, to aerodynamic phenomena, to periodic recurrences of economic crises and epidemics, to plasma relaxation oscillations, to the relaxing charge-discharge of musical instrument strings (Botero et al., 2012).

Oscillatory processes are important in modelling and studying dynamical plasma structures. Theoretically, the solution of Maxwell's equations in systems with charge sources predicts characteristic oscillations. If the mechanisms of creation and assimilation of charges as well as the coupling of their movement with electromagnetic fields enable a negative friction with a term that satisfies the general Lienard conditions, the system develops typical relaxation oscillations, and the oscillation converges to a limit cycle. Since this process is very complicated, numerical integration is fundamental in the study of the phenomenon. Accordingly, such behaviour appears in the advancement of combustion in optical fibres as well as in some processes in charged interstellar dust, etc. Numerical study in this case is very important as it enables the interpretation of the phenomenon, recognition of specific conditions when the phenomenon occurs as well as the reverse use for application purposes.

Classical Approximation of the Equations of Motion for the Two-Fluid System

The force exerted on a charged particle moving in an electromagnetic field is given by the Lorentz equation:

$$\boldsymbol{F} = q_\alpha(\boldsymbol{E} + \boldsymbol{v} \times \boldsymbol{B}) \rightarrow m_\alpha \frac{d\boldsymbol{v}}{dt} = q_\alpha(\boldsymbol{E} + \boldsymbol{v} \times \boldsymbol{B}). \quad (1)$$

Where α defines the type of particle electron or ion, thus defining 2 different equations for 2 different fluids, one of ions and the other of electrons. Instead of the velocity v of a particle, we use the average velocity u and multiply both sides by the charge density $n_{\alpha 0}$ (Chen, 1984):

$$m_\alpha n_{\alpha 0} \frac{d\boldsymbol{u_\alpha}}{dt} = q_\alpha n_{\alpha 0}(\boldsymbol{E} + \boldsymbol{u_\alpha} \times \boldsymbol{B}). \quad (2)$$

The force of the pressure gradient is also present in plasma. In the approximation of fluids, the time derivative in (2) is written as a convective derivative (Chen, 1984; Maiorov et al., 1992) and the relation is:

$$mn_{\alpha 0}\left[\frac{\partial \boldsymbol{u_\alpha}}{\partial t} + (\boldsymbol{u_\alpha} \cdot \nabla)\boldsymbol{u_\alpha}\right] = qn_{\alpha 0}(\boldsymbol{E} + \boldsymbol{u_\alpha} \times \boldsymbol{B}) - \nabla P. \quad (3)$$

Collisions between different particles enable the exchange of energy between them. Dispersion affects the amount of movement of a type of particle such as an electron, ion or neutral particle. The rate of momentum loss from collisions between particles, of type α and neutral particles or between the same type is given by $R_{\alpha k} = \nu_{\alpha k} n_\alpha m_\alpha(\boldsymbol{v_\alpha} - \boldsymbol{v_k})$, and is obtained (Goldston & Ratherford, 2000):

$$m_\alpha n_{\alpha 0}\left[\frac{\partial \boldsymbol{u_\alpha}}{\partial t} + (\boldsymbol{u_\alpha} \cdot \nabla)\boldsymbol{u_\alpha}\right] = q_\alpha n_{0\alpha}(\boldsymbol{E} + \boldsymbol{u_\alpha} \times \boldsymbol{B}) - \nabla P - \nu_{\alpha k} n_{\alpha 0} m_\alpha(\boldsymbol{u_\alpha} - \boldsymbol{u_k}). \quad (4)$$

In fact, the dispersion of charged particles with neutral particles is a type of viscosity that appears to the liquid. The term $(u_\alpha \cdot \nabla)\, u_\alpha$ is argued to be negligible in (Chen, 1984) where u_α is assumed to be so small that this quadratic term is negligible.

Considering the equation of state $pn^{-\gamma}$=constant for any gas, and if we consider it as an isothermal process then γ takes the value 1, but we have thermal exchange, so we must consider it. If we define the pressure and density as $P=p_0+p_1$ and $n=n_0+n_1$ where p_0 and n_0 represent the constant pressure and density while p_1 and n_1 represent the turbulent part, we can write the equation considering an isothermal background $P_0=n_0kT$ from which we arrive at another relation between P and n as follows (Lankin, & Norman, 2009; Chen, 1984; Smirnov, & Boris, 2001):

$$\frac{\nabla P}{p_0} = \gamma \frac{\nabla n_{1\alpha}}{n_0}, \quad (5)$$

from which we conclude:

$$\nabla P = \gamma kT \nabla n_{1\alpha}, \quad (6)$$

If we consider the charge distribution according to the Boltzman distribution, we will get the "disturbance scale". If we decompose it into Taylor series, we will see that we have a perturbative term, which will represent the variable part of the density of electrons or charges in general, so n_0 represents the constant part while n1 represents the variable part and $nq= n_0+n_1$ (McGreivy, 2017; Hafeez, & Ndikilar, 2014)):

$$n_q = n = n_0 e^{e\Phi/kT_e} = n_0\left(1 + \frac{e\Phi}{kT_e} + \ldots\right) = n_0 + n_0\frac{e\Phi}{kT_e} + \cdots \quad (7)$$

then, we can find the ratio $\frac{n_1}{n_0} = \frac{e\Phi}{k_B T_e}$, where e is the electron charge, Φ is the potential, k_B is the Boltzmann constant, and T_e is the electron temperature. After replacing the equations in equation (4) and doing the divergence of this equation we get:

$$m_\alpha n_{0\alpha} \nabla \cdot \frac{\partial \boldsymbol{u}}{\partial t} = q_\alpha n_{0\alpha} \nabla \cdot \boldsymbol{E} + q_\alpha n_{0\alpha} \nabla \cdot (\boldsymbol{u} \times \boldsymbol{B}) - \gamma k_B T \nabla^2 n_{1\alpha} - \nabla\big(\nu n_{0\alpha} m_\alpha(\boldsymbol{u_\alpha} - \boldsymbol{u_k})\big). \quad (8)$$

Since the mass of electrons is very small, we will consider the dynamic equation only for one of the types of particles, i.e. for ions, although we can combine both equations for each type of particle and arrive at the same point again. We chose the first path. (Below we will eliminate the index α, implying that the equation is written for ions). The equation takes the form:

$$\nabla\cdot\frac{d\boldsymbol{u}}{dt}-\frac{q}{m}\nabla\cdot\boldsymbol{E}-\frac{q}{m}\nabla\cdot(\boldsymbol{u}\times\boldsymbol{B})+\frac{\gamma k_B T}{mn_0}\nabla^2 n_1+\frac{1}{n_0 m}\nabla(\nu n_0 m(\boldsymbol{u}-\boldsymbol{u_k}))=0. \tag{9}$$

The electric field is given as the gradient of the potential with a minus sign in front, and the velocity of the particles entering the scattering can be taken to be 0 or incorporated together into a velocity u:

$$\nabla\cdot\frac{d\boldsymbol{u}}{dt}+\frac{q}{m}\nabla^2\Phi-\frac{q}{m}\nabla\cdot(\boldsymbol{u}\times\boldsymbol{B})+\frac{\gamma kT_i}{mn_0}\nabla^2 n_1+\nu\nabla\cdot\boldsymbol{u}=0. \tag{10}$$

Substituting Φ we get:

$$\nabla\frac{d\boldsymbol{u}}{dt}+\frac{k_B}{n_0 m}(T_e+\gamma T_i)\nabla^2 n_1-\frac{q}{m}\nabla\cdot(\boldsymbol{v}\times\boldsymbol{B})+\nu\nabla\cdot\boldsymbol{u}=0. \tag{11}$$

We try to derive the continuity equation with respect to time:

$$\frac{\partial S}{\partial t}=\frac{\partial}{\partial t}\left(\frac{\partial n_1}{\partial t}+n_0\nabla\cdot\boldsymbol{u}\right)=\frac{\partial^2 n_1}{\partial t^2}+n_0\nabla\cdot\frac{\partial\boldsymbol{u}}{\partial t}. \tag{12}$$

We substitute the time derivative of the velocity divergence:

$$\frac{dS}{dt}-\frac{d^2 n_1}{dt^2}+\frac{k_B}{m}(T_e+\gamma T_i)\nabla^2 n_1-\frac{qn_0}{m}\nabla\cdot(\boldsymbol{u}\times\boldsymbol{B})+\nu\left(S-\frac{dn_1}{dt}\right)=0, \tag{13}$$

from where:

$$\frac{dS}{dn_1}\frac{dn_1}{dt}-\frac{d^2 n_1}{dt^2}+\frac{k_B}{m}(T_e+\gamma T_i)\nabla^2 n_1-\frac{qn_0}{m}\nabla\cdot(\boldsymbol{u}\times\boldsymbol{B})+\nu S-\nu\frac{dn_1}{dt}=0. \tag{14}$$

We will assume that the potential is harmonic in space, so $\phi(z,t)=\phi(t)e^{-ikr}$ where k is the wavenumber of the harmonic potential. If we do the Laplacian of the potential, we get $\phi(z,t)=-k^2\phi(t)$. Since the potential is directly proportional to the charge density n1 then the same phenomenon will occur with the density under the effect of the harmonic potential. Thus $\nabla^2 n_1=-k^2 n_1$. Substituting the source term we get (B. Keen, & E. Fletcher, 1970):

$$\begin{aligned}(\alpha-2\beta n_1-3\xi n_1^2)\frac{dn_1}{dt}-\frac{d^2 n_1}{dt^2}-\frac{k_B k^2}{m}(T_e+\gamma T_i)n_1-\frac{qn_0}{m}\nabla\cdot(\boldsymbol{u}\times\boldsymbol{B})\\+\nu(\alpha n_1-\beta n_1^2-\xi n_1^3)-\nu\frac{dn_1}{dt}=0.\end{aligned} \tag{15}$$

From the above formula, considering the geometric configuration for which the density changes according to x, so the electrons move according to x while the magnetic field oscillates according to y then we can write:

$$\nabla\cdot(\boldsymbol{u}\times\boldsymbol{B})=\begin{vmatrix}\partial_x & \partial_y & \partial_z\\ u_x & 0 & 0\\ 0 & B_y & 0\end{vmatrix}=\partial_z u_x B_y=0. \tag{16}$$

The equating to 0 of the above derivation comes from considering that the magnetic field and velocity vary very little in other directions. Thus, obtaining the equation:

$$(\alpha-\nu-2\beta n_1-3\xi n_1^2)\frac{dn_1}{dt}-\frac{d^2 n_1}{dt^2}-\frac{k_B k^2}{m}(T_e+\gamma T_i)n_1+\nu\alpha n_1-\nu\beta n_1^2-\nu\xi n_1^3=0. \tag{17}$$

If the scattering between different types of particles and neutral particles is dominant our equation does not tend to the Van der Pol relaxation oscillator but arrives at the Van der Pol-Dufing (the equation above), which modified by external excitations, the system approaches chaos (Enjieu Kadji et al., 2008; Miwaddinow et al.. 2013). In special cases when this does not happen, i.e. when ν≃0 the system tends towards approximately Van der Pol oscillation:

$$\frac{d^2n_1}{dt^2} - (\alpha - 2\beta n_1 - 3\xi n_1^2)\frac{dn_1}{dt} + \omega_0^2 n_1 = 0, \tag{18}$$

where ω is the plasma frequency:

$$\omega_0^2 = \frac{k_B k^2}{m}(T_e + \gamma T_i). \tag{19}$$

In specific cases relation 18 returns to the standard form of the VdP (Van der Pol) oscillator which justifies the experimental findings.

Fiber Fuse

The problems that appeared in the production of fibres, because of the loss of homogeneity, that is, the creation of impurities in the fibres, have brought physical, local phenomena, which can affect the purity of the signal.

Impurities created during production and defects (such as Frenkel defects, Si E' and Ge E' centres) appearing after production, occurring in the path of the electromagnetic wave, cause absorption, scattering, and therefore temperature increase. According to studies (Shuto), the increase in temperature causes an increase in absorbance in silica glass while the increase in absorbance causes an increase in temperature so we get into a chain effect. After a critical value of temperature, the glass will start to melt. With further increases in temperature, ionization and a series of other consecutive phenomena begin, thus initiating the formation of a local micro plasma, whose charge density begins to oscillate according to the Van der Pol oscillator (Shuto, 2018).

Oscillating charge density will result in a variable refractive index which affects signal transmission. The formed plasma moves towards the laser source at a speed of the order of meters per second. This phenomenon is known as Fiber Fuse or fibre burning. What remains after the fuse is a series of cavities. The cavities formed do not allow the direction of light, so the fibre becomes useless. In the following, we will try to model this phenomenon using the Van der Pol oscillator. An interesting observed characteristic of a fibre fuse is the propagation of a bright spot towards the laser source.

The propagation speed of the fibre fuse is generally of the order of meters per second and increases almost linearly with the pump laser power. After the fibre has burned out, a series of bullet-shaped cavities are left behind, and the fibre is no longer able to guide light. Figure 1 shows an example of damage; a burning of fibres spreading from right to left.

Figure 1. "Fiber Fuse" propagation phenomenon for laser power a) 1.2W b) 3.5W, c) 7W decreasing from (c) to (b) and finally to (a) where progress is stopped (Yakovlenko, 2006)

Van der Pol Modelling of Plasma Oscillation in Optical Fibres

Referring to equation 17 where we derived the plasma oscillation equation in physical systems, we manage to derive an approximate equation in the Van der Pol model for plasma oscillation in optical fibres.

Summarizing the terms and rescaling we get:

$$\frac{d^2\mathrm{N}}{dt^2} - \mathrm{f(N)}\frac{d\mathrm{N}}{dt} + \mathrm{g(N)} = 0 \tag{20}$$

If in 20 the functions f(N) and g(N) satisfy the Lienard conditions (Strogatz, 2003) the system can undergo a Hopf bifurcation, and the rescaled parameter performs relaxation oscillations where the increase of the amplitude above a threshold leads to its decrease and vice versa. The necessary condition for this is that f(N) is an even function and g(N) is odd. These conditions would be obtained if the constants included in the original equation derived within the approximations made (classical approximation of cold plasma with stationary distribution) and which in principle, according to the preceding discussion, are obtained from effective sections and shock frequencies with ionization consequences and cargo reunification, take on special values.

The laser effect on plasma dynamics is not only present at the instant of plasma creation as an initiator along with defects, but it acts on the plasma even after its formation. The influence of the laser on the plasma is indirect, since its power is small, the laser will only affect the temperature of the front part of the FF (fibre fuse). When the laser is more powerful the impact will be direct. Thus, modelling the laser impact of the form $F_0 cos\omega t$ as an external impact, where ω is the external frequency and F_0 is the amplitude of the external excitation, we arrive at approximately the forced Van der Pol-Duffing equation (Miwadinou et al., 2013):

$$\frac{d^2n_1}{dt^2} - (\alpha - \nu - 2\beta n_1 - 3\xi n_1^2)\frac{dn_1}{dt} + \omega_0^2 n_1 + \nu\alpha n_1 - \nu\beta n_1^2 - \nu\xi n_1^3 = F_0 cos\omega t \tag{21}$$

In the simulations we will do, we will see how the particle density behaves under special conditions when the parameter $\nu \simeq 0$, i.e. the plasma modelled for low scattering frequency between 2 fluids and for weak laser effect, for which the system behaves purely as a Van der Pol oscillator. We will also see how the system behaves when we consider $\nu \neq 0$ and the laser effect is dominant.

It has been experimentally proven that for cases where the laser is more powerful than usual, the burning of the optical fibre is even more catastrophic, in the sense that what remains after the burning is simply a destruction of the optical fibre. In this context, we expect that for large values of the external excitation force, the behaviour of the system will be quasi-chaotic.

Numerical Integration of Plasma Oscillation in Optical Fibres

The oscillation of the plasma charge density in optical fibres based on the solution of the plasma equations is the relaxation oscillation characterized by slow charging and fast discharging of the Van der Pol oscillator-like system. If we do the 'normative' substitutions or transitions in the natural parameters and variables of the system:

$$\varepsilon = \alpha - \nu, \quad \tau = \omega_0 t, \quad n_1 = \sqrt{\frac{\varepsilon}{3\xi}}n, \quad \gamma = \frac{2\beta}{\varepsilon}\sqrt{\frac{\varepsilon}{3\xi}}, \quad \mu = \frac{\varepsilon}{\omega_0},$$
$$k_1 = \frac{\nu\alpha}{\omega_0^2}, \quad k_2 = \sqrt{\frac{\varepsilon}{3\xi}}\frac{\nu\beta}{\omega_0^2}, \quad k_3 = \frac{\varepsilon}{3}\frac{\nu}{\omega_0^2}, \quad F = \sqrt{\frac{3\xi}{\varepsilon}}F_0, \quad \Omega = \frac{\omega}{\omega_0}. \tag{22}$$

We get the equation:

$$\frac{d^2n}{d\tau^2} - \mu(1 - \gamma n - n^2)\frac{dn}{d\tau} + n - k_1 n + k_2 n^2 + k_3 n^3 = F cos\Omega\tau \tag{23}$$

where n represents the parameterized density.

Empirical Estimation of Relaxation Oscillation Conditions

In the study of burning fibres, the situation of the appearance of bubbles with dimensions of several micrometres that in different conditions have different sizes and periodicities was observed and photographed. The interpretation of the phenomenon is intended as a jump of the generated plasma system in an oscillatory state of relaxation. In fact, the classical equation for γ=0, k1,2,3=0, and F=0 is exactly the Van der Pol model:

$$\frac{d^2n}{d\tau^2} - \mu(1-n^2)\frac{dn}{d\tau} + n = 0. \qquad (24)$$

Physically, $\gamma n \ll 1$, $(1-\gamma n - n^2) \sim (1-n^2)$i.e. $\gamma \ll \frac{1}{n}$ i.e. $\gamma = \frac{2\beta}{\varepsilon}\sqrt{\frac{\varepsilon}{3\xi}} \ll \frac{1}{n}$ where n is the density normed. One-by-one identification of these parameters is possible within these calculations and numerical verification would validate the interpretive model here. In the referenced literature, it is assumed that these conditions are met, while we numerically generate alternatives because such connections do not appear directly. The confirmation of the transition to self-contained oscillatory states is taken as evidence of the validity of the model that gives the origin of the phenomenon, despite keeping the parameters in their original form, after renormalization.

To integrate it in MATLAB (Böttcher, 2000; Nicolas Girodano, & Hasao Nakanishi, 2005) we will have to replace n=y_1 and transform it into the form of 3 differential equations to implement it in the ode package:

$$\dot{y}_1 = y_2 \qquad (25)$$

$$\dot{y}_2 = \mu(1-\gamma y_1 - y_1^2)y_2 - y_1 + k_1 y_1 - k_2 y_1^2 - k_3 y_1^3 + Fcos(\Omega y_3) \qquad (26)$$

$$\dot{y}_3 = 1 \qquad (27)$$

Terminology and Graphic Presentation

We have performed all the relevant calculations even though we are not presenting them here, starting with some axioms or assumptions. Each of them requires special attention and comment. The findings of the literature (Shuto, 2020; Yakovlenko, 2005) are not fully reconfirmed in our complementary treatment, but by the very nature of the treatment, we will not be interested in conditions that lead to the validity of the assumptions that bring about the pure VdP form but will simulate scenarios that improvise those conditions and see the behaviour of the charge density. Oscillations of the charge density in the environment immediately lead to the appearance of a spatial oscillation, accepting that the process takes place on the surface of the created bubble and consequently propagates toward the source. The approximation is that the propagation speed is constant, and the screening effects studied above act as described. Then, in our presentation, we will consider the normalized parameters, and their physical meaning will be read in the set of parametrization equations 23. In the following simulations referring to the parametrizations made and studies (Shuto, 2021) taking the frequency of the plasma of the order of MHz, the time will be of the order of µs. A more accurate analysis requires an interpretation within the framework of electrodynamics. quantum s from which we can derive a more accurate form of the values of the ionization and recombination frequencies. However, referring to studies (Shuto, 2020) the density of the charge is of the order of 10^{20} units of particles/m^3.

Simulation for very small γ and k1,2,3

Initially, we assumed the values γ≃0 and $k_{1,2,3}$, ≃0 (for the case when the external influence is small F=0) according to parametrizations and numerically integrated the equations.

In the figure below, the system behaves like a Van der Pol oscillator where the nonlinearity parameter μ takes the value 1.

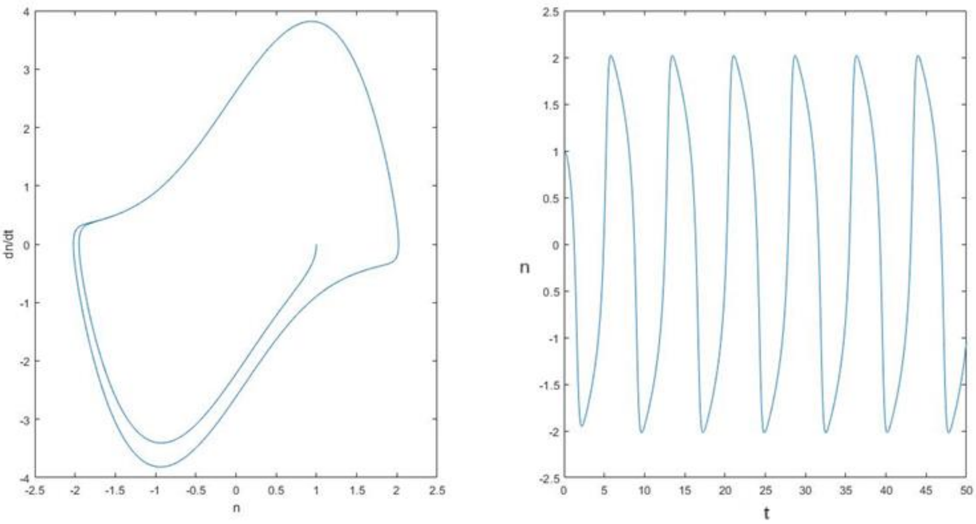

Figure 2. Phase portrait and oscillation for μ=2

In Figure 4 we have presented the oscillation of the charge density in relation to time for different values of the parameters ranging from -1 to 2 with a step of 0.2, this is also reflected in Figure 5 of the phase portrait. As can be seen in the figure, for negative values of μ, the system has a solution according to a stable spiral, which disappears as quickly as the nonlinearity parameter is smaller. For parameter 0 we reach the harmonic oscillator, and for larger values, we reach the Van der Pol oscillator. We see that with a further increase of the nonlinearity parameter, the oscillation period of the plasma charge density increases.

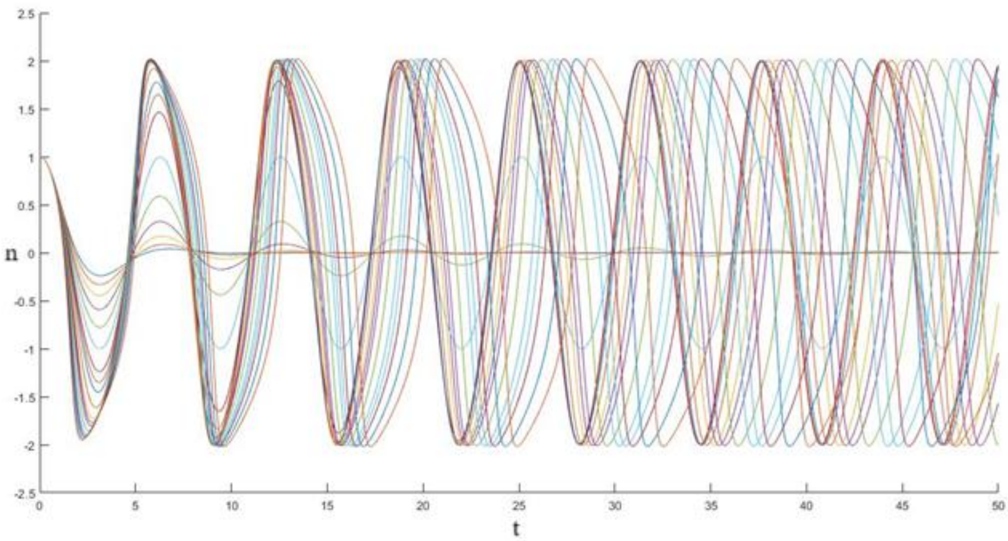

Figure 3. Oscillation of the normalized charge density for different values of the parameter μ from -1 to 2 with a step of 0.2 (ie for μ=-1,-0.8,-0.6,….1.6,1.8,2)

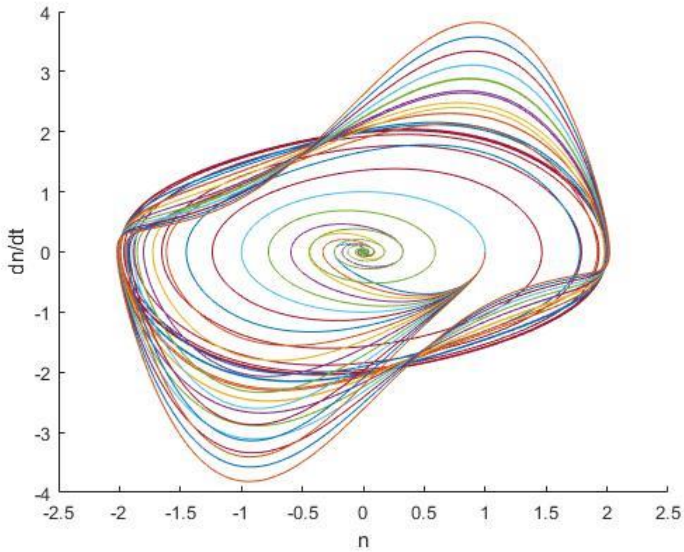

Figure 4. Phase space, limit cycles and stable spirals for μ from 1 to 2 with step 0.2

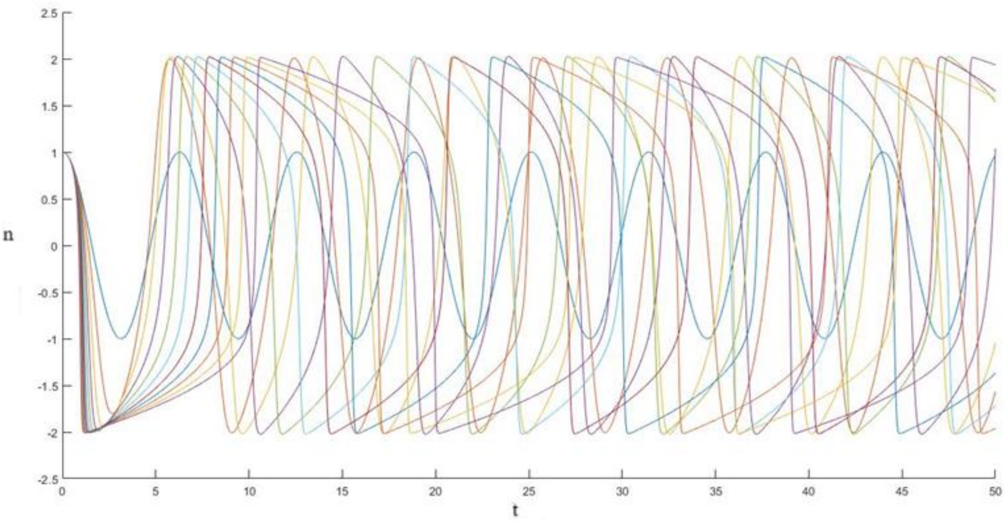

Figure 5. Oscillation of charge density for μ from 0 to 10 with step 1

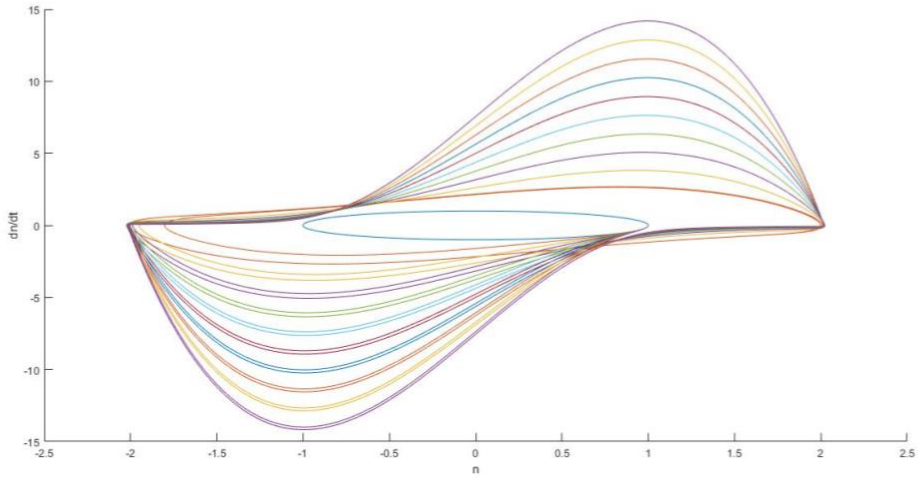

Figure 6. Limit cycles for μ from 0 to 10 with step 1

Referring to Figures 5 and 6 where μ has a wider range of values (from 0 to 10 with step 1 practically 0, 1, 2....9, 10) we see that for large values of the parameter μ, the nonlinearity comes and is accentuated, and the period takes ever larger values for the largest nonlinearity parameter.

General modelling, γ≠0

First, we fix the parameter μ=1 and give different values to the parameter γ as we will see in the following figures. For larger values of γ in Figures 8 and 9 we see that the deformation is larger introducing a broadening in the upper part of the limit cycle reflected in a sharpening of the charge density oscillation.

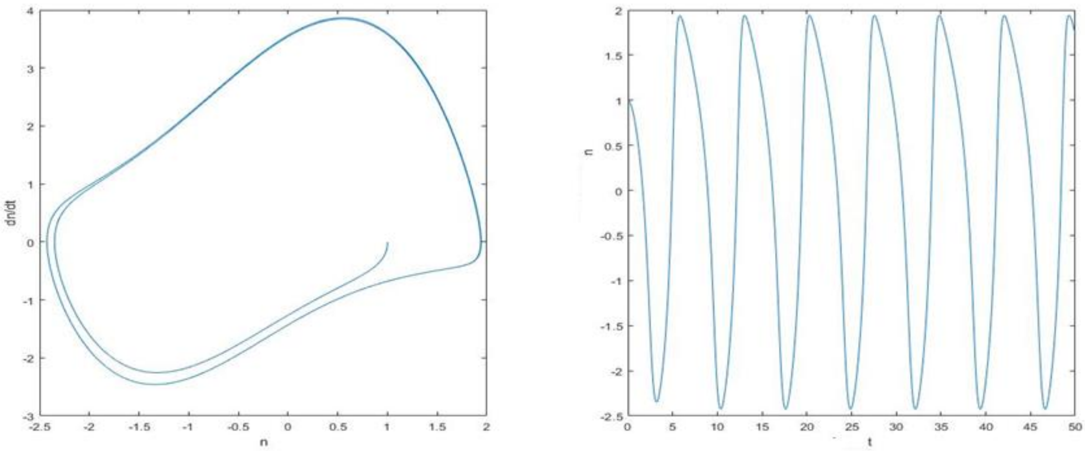

Figure 7. Limit cycle and charge density oscillation for fixed μ=1 and for γ=1

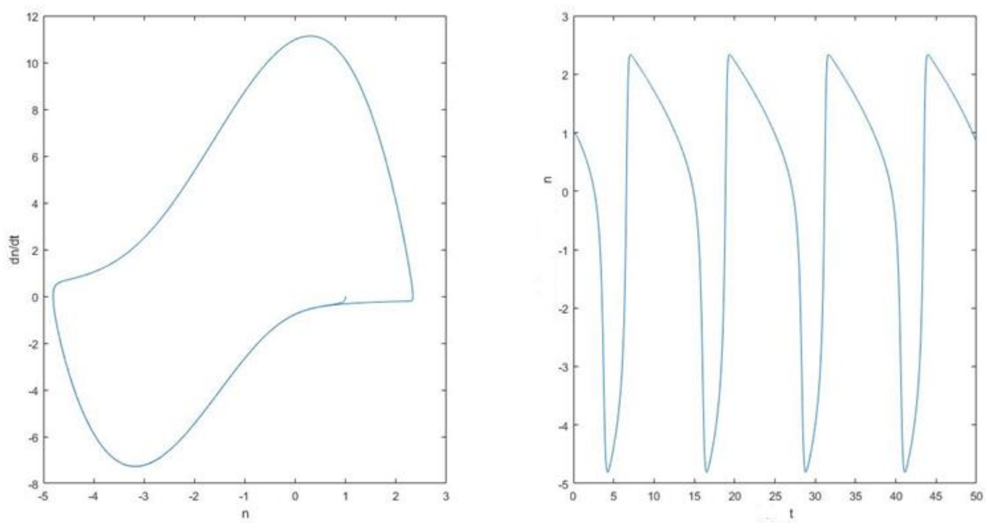

Figure 8. Limit cycle and charge density oscillation for fixed μ=1 and for γ=3

Change in relaxation amplitude

The simulation shows that the amplitude of the oscillation varies depending on other conditions. We note that in the approximation of the harmonic oscillator, the constant amplitude is given by the invariance of the axes of the ellipse, while in our cases, the stability of the phase portrait indicates that the amplitude is variable and corresponds to that limit cycle.

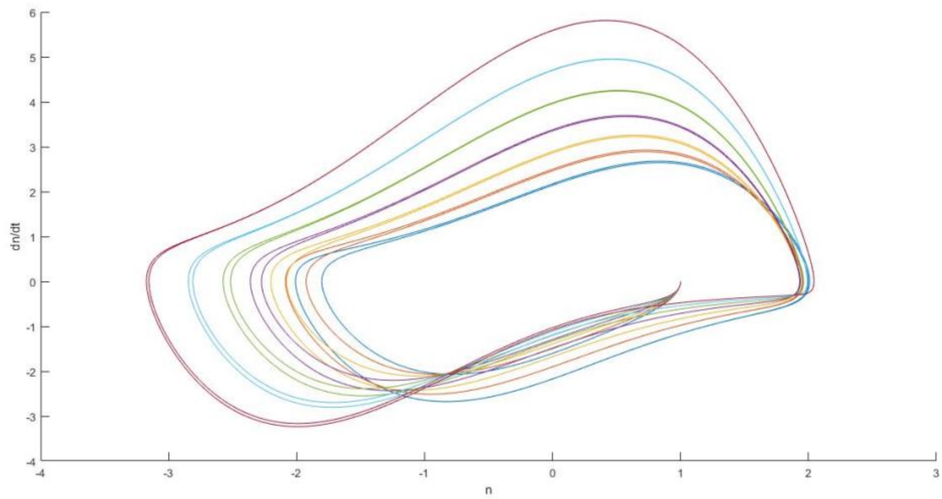

Figure 9. Limit cycles for μ=1 fixed and for γ varying from 0 to 2 with a step of 0.3

Now we produce a new scenario, we change the parameter γ which is related to $\gamma = 2\beta\sqrt{\frac{1}{3\varepsilon\xi}}$ .The diagram shows that the phase portrait changes, which shows that the amplitude changes. This change is not exactly a quenching-type effect, since the trajectory does not self-assemble, but a resizing self-copy and some subsequent deformation is observed. Referring to Figures 11 and 12 where we have shown the phase space and the solution of the equation for fixed μ and for γ that varies from 0 to 2 with a step of 0.3, we understand that the limit cycle expands the larger the be parameter γ. Also, as the parameter increases, the amplitude and period increase.

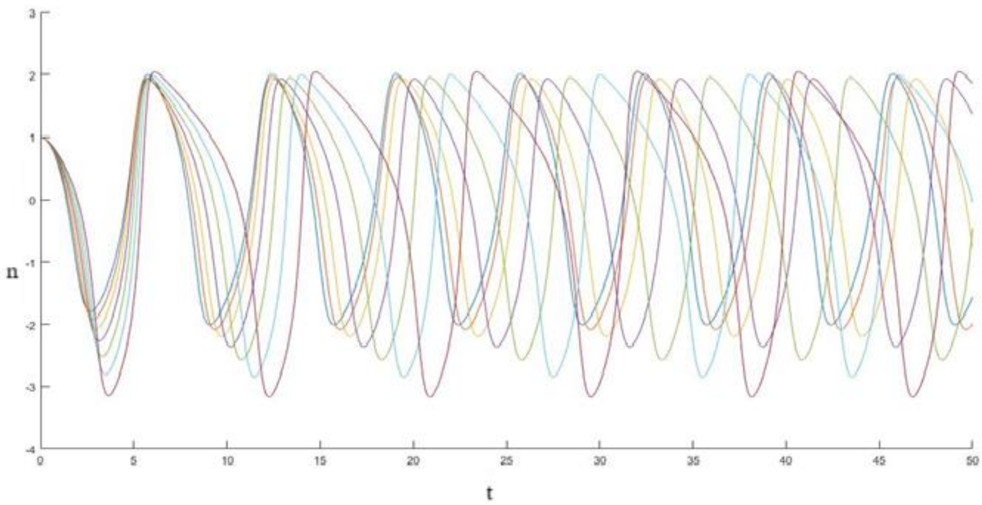

Figure 10. Charge density oscillation for fixed μ=1 and for γ varying from 0 to 2 with step 0.3

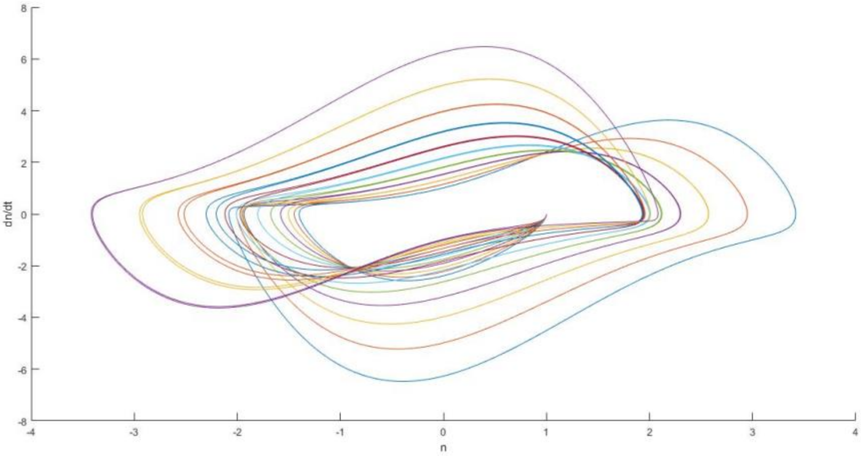

Figure 11. Limit cycles for μ=1 fixed and for γ varying from -2 to 2 with step 0.4

This behavior indicates that it differs from the previous regime by moving away from that of relaxation. In Figure 13, we have simulated the same model for a fixed nonlinearity parameter but for γ that varies from negative to positive values where, as we see from the figure, the implementation of negative values of the parameter gives us expansion/deformation in the lower part of the limit cycle.

As the parameter γ increases from -2 to 2, we see that the system passes from an oscillator with lower amplitude (for γ=-2) through a Van der Pol oscillator, for parameter 0, to an oscillator with upper amplitude (for γ= 2).

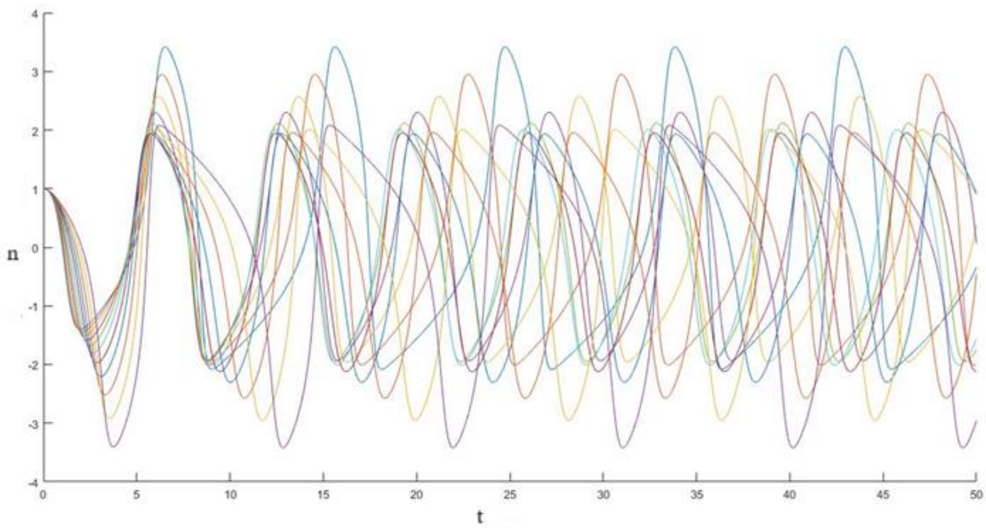

Figure 12. Charge density oscillation for fixed μ=1 and for γ varying from -2 to 2 with step 0.4

Unstable and chaotic regimes

In this case, we considered γ≠0, k1,2,3, ≠0 and the external influence F≠0. We will see that the system will not oscillate according to one relaxing oscillation but will follow oscillations and near-chaotic behaviour. We first try to give these values γ=1, k1=0, k2=3.05, k3=1.5, F=1, Ω=1 (Miwadinou et al., 2013; Kadji et al., 2008) and do the simulation for different values of the nonlinearity parameter of the Van der model Pol, μ, and we see how the phase space depends.

We see that for small values of the μ parameter, the behaviour is oscillatory and quite slow. For larger values of the parameter μ the system spirals towards a fixed point. We are interested in studying the behaviour of the system for small values of the parameter μ to understand more details of this limit. The laser effect on plasma in optical fibres is an external factor that can be controlled by us more than any other parameter in the dynamic equation. Thus, in the following 2 figures we have presented the phase space and the charge density oscillation by fixing the parameters $\mu=0.02$, $\gamma=1$, $k_1=0$, $k_2=3.05$, $k_3=1.5$, $\Omega=0.5$ and for 2 different values of F.

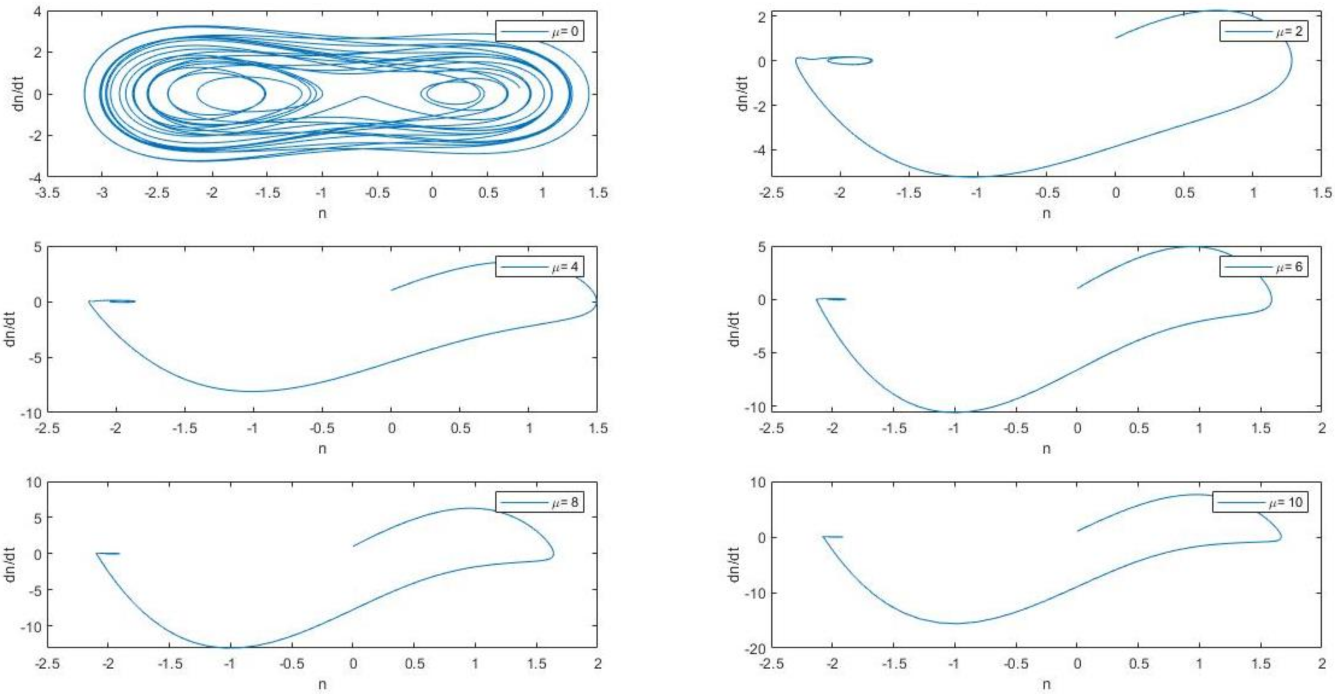

Figure 13. Phase space $\gamma=1$, $k_1=0$, $k_2=3.05$, $k_3=1.5$, $F=1$, $\Omega=1$ and for 6 different values of μ from 0 to 10

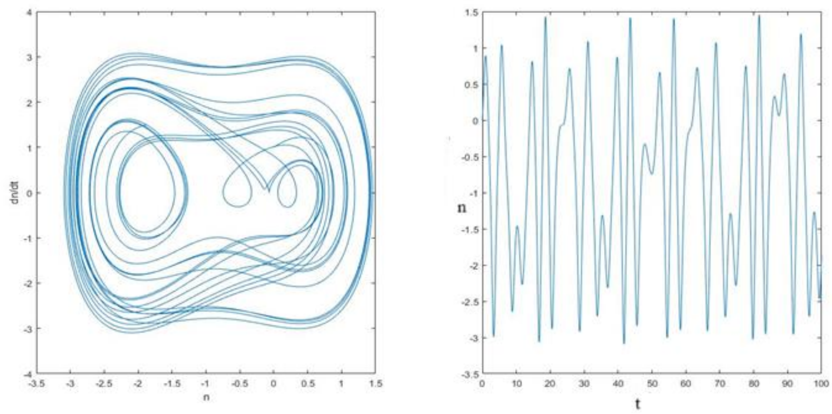

Figure 14. Phase space and charge density oscillation for $\mu=0.02$ $\gamma=1$, $k_1=0$, $k_2=3.05$, $k_3=1.5$, $\Omega=0.5$ and $F=3.4$

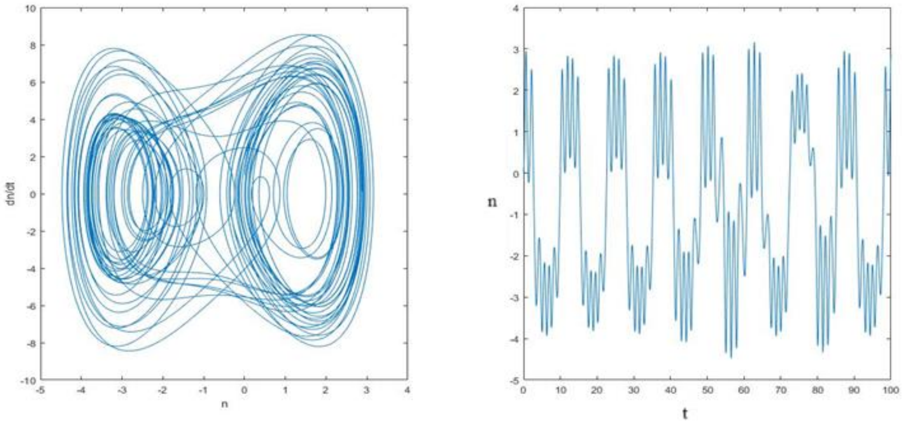

Figure 15. Phase space and charge density oscillation for μ=0.02, γ=1, k_1=0, k_2=3.05, k_3=1.5, Ω=0.5 and F=20.5

We see that for different values of F, the behaviour of the system changes, so we need to study how the parameter F affects the chaotic behaviour of the system.

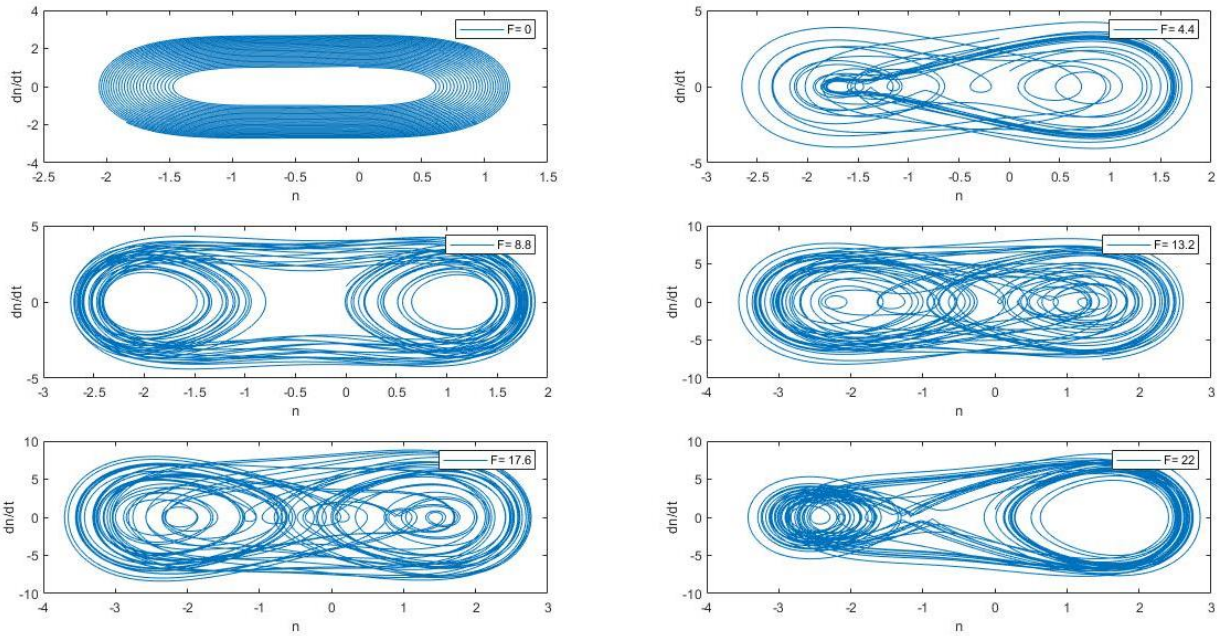

Figure 16. Phase space for values μ=0.02, γ=1, k_1=0, k_2=3.05, k_3=1.5, Ω=0.5 and for F ranging from 0 to 22

As we see from Figures 18 and 19 for F close to 0 the system is close to a limit cycle but, in this case, the system is spiralling unstable but with a small growth rate, i.e. the system diverges "slowly". For F>0 the system exhibits a quasi-chaotic behaviour spiralling sometimes on one side and sometimes on the other side of the phase space in an irregular manner.

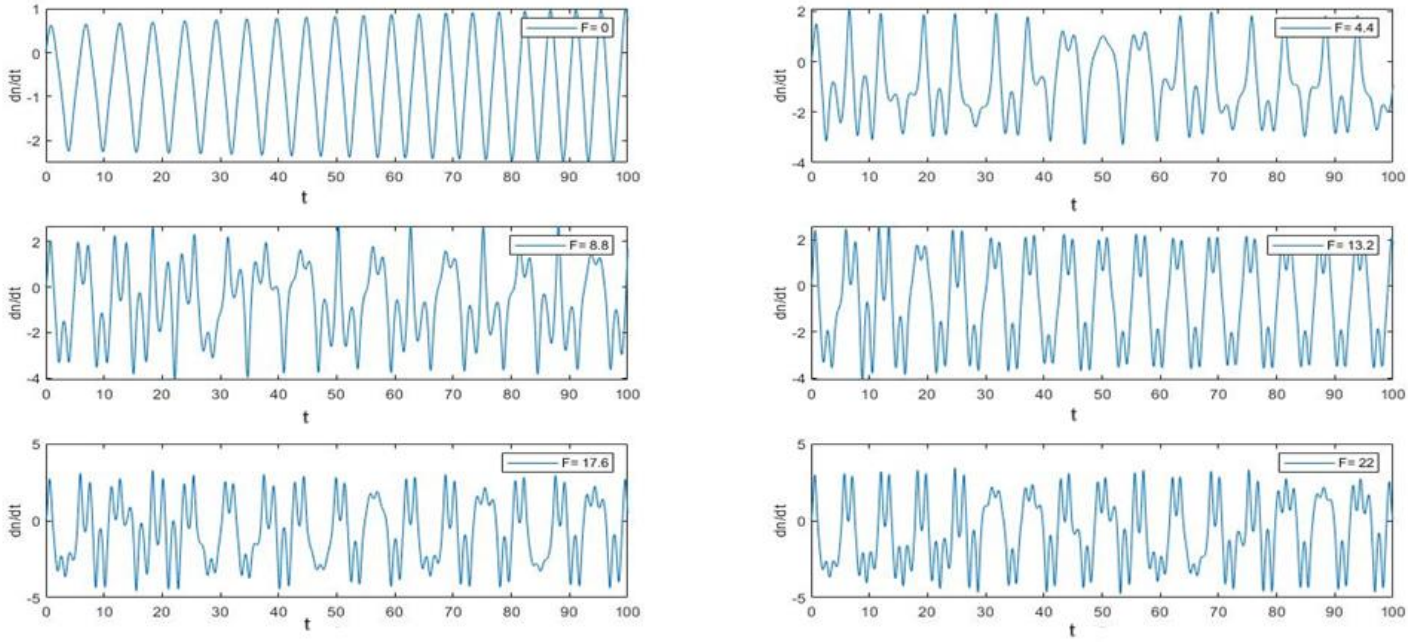

Figure 17. Charge density oscillation for μ=0.02, γ=1, k_1=0, k_2=3.05, k_3=1.5, Ω=0.5 and for F varying from 0 to 22

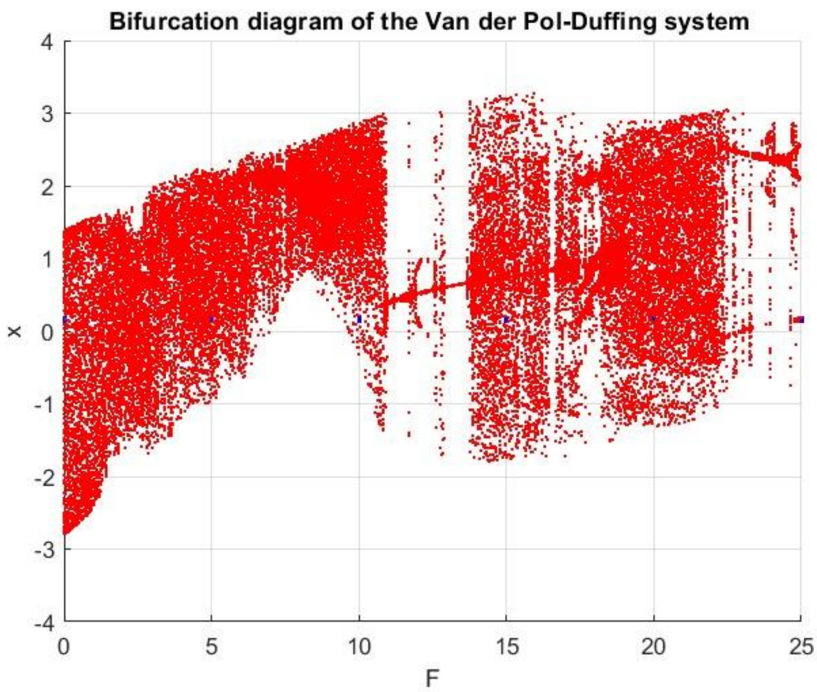

Figure 18. Bifurcation diagram for μ=0.02, γ=1, k_1=0, k_2=3.05, k_3=1.5, Ω=0.5, and for F varying from 0 to 25

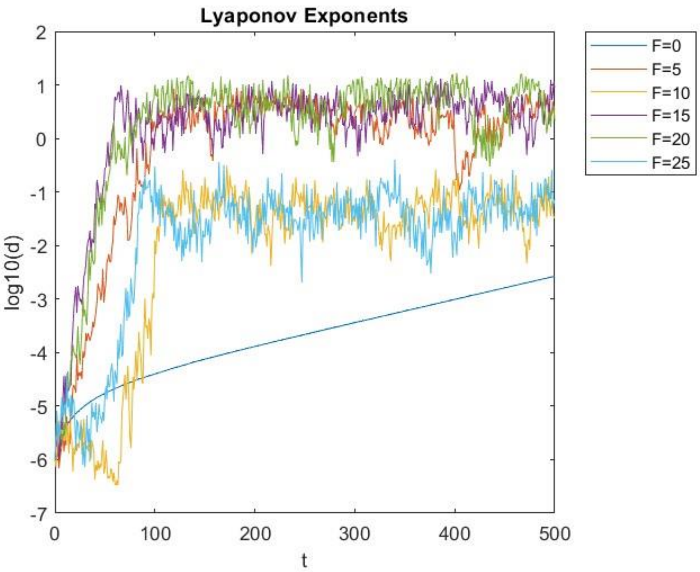

Figure 19. Lyaponov exponents for F from 0 to 25

Figure 18 shows the bifurcation diagram for different values of the parameter F, where it is seen that the system undergoes chaotic behaviour for most cases of F, except for specific points. This diagram is simulated by numerically integrating the system and simulating the Poincare maps from which the bifurcation diagram is derived.

Figure 19 shows the Lyapunov exponents for which approximate initial values were considered from which the internalization started (Biswa, 2007; Gega et al.,2024). Lyapunov exponents are added geometrically between them. As can be seen in each of the cases under consideration, the exponents are positive, which fulfils one of the conditions of chaos, being sensitive to the initial conditions.

Conclusion

The relaxation oscillation, according to the assumptions made, will not only occur in time but also in space along the fibre axis. The shape of the remaining cavities is a consequence of this oscillation along the fibre axis. For the case of fuse in optical fibres, when the propagation frequency between fluids and one of the frequencies in the nonlinear continuity equation are very small $k1,2,3 \simeq 0$, $\gamma \simeq 0$ (normalized parameters) the system has a regular and relaxing Van der Pol oscillatory behaviour.

From the simulation of the charge density oscillation with respect to time for the case of plasma oscillation in optical fibres (exact VdP model) for $\gamma \simeq 0$ we observe an increase in the period with increasing nonlinearity parameter. The dependence between the nonlinearity parameter and the period is determined according to the figure below.

When $\gamma \neq 0$ the model is not Van der Pol but an approximate model of it. This model exhibits some deformation in the amplitude and period of the oscillation and in the components of the period. According to the direct proportion between the spatial and temporal period (in the approximation when the burning rate is constant) and since the distance between the cavities and the length of the cavity are not equal (measured), this form of the oscillation model is more acceptable than the exact Van der Pol form.

We see that the amplitude of the oscillation increases mainly. This effect comes from the introduction of the term γ. For negative values of the parameter γ the reverse process occurs.

In the case when $k1,2,3 \neq 0$, the system will be quite confused. If we consider an external influencing term the system will reach quasi-chaotic behaviour. The laser was simply the initiator of the plasma, and its influence is hidden in the plasma temperature and in other parts since its energy is of the order w. A powerful laser, for example of the order kw, would have a direct influence on the particle density, therefore the external exciting term can be seen as an energetic laser. Experiments performed under such conditions show us a “bad” burning of the fibre or a “messy” burning (Frolov et al., 2006), i.e. without periodic cavities, a factor that gives us an indication that the behaviour in these cases may be quasi-chaotic.

Plasma relaxation oscillations have found engineering applications such as in Tokamaks, cavity sensors caused by fibre fuse, etc. The consequences caused by plasma relaxation oscillations in optical fibres have found efficient and economical applications in the field of sensors (Domingues et al., 2015; Rao et al., 2017)

References

Biswa, D. (2007). Model Updating and Simulation of Lyapunov Exponents. *Proceedings of the European Control Conference* (pp. 1094 - 1100). Kos, Greece.

Botero, W. A., Salas, A. H., & Colorado, S. J. G. (2013). The Hodgkin-Huxley neuron model on the fast phase plane. *International Journal of Physical Sciences*, *8*(20), 1049-1057.

Böttcher, D. L. (2000). Introduction to Computational Physics.

Chen, F. F. (1984). Plasma Physic and Controlled Fusion.

Enjieu Kadji, H. E., Chabi Orou, J. C., & Woafo, P. (2008). Regular and chaotic behaviors of plasma oscillations modeled by a modified Duffing equation. *Physica Scripta*, *77*(2), 025503.

Enjieu Kadji, H. G., Nana Nbendjo, B. R., Chabi Orou, J. B., & Talla, P. K. (2008). Nonlinear dynamics of plasma oscillations modeled by an anharmonic oscillator. *Physics of Plasmas*, *15*(3).

Frolov, A. A., Bufetov, I. A., Efremov, V. P., Schelev, M. Y., Lozovoy, V. I., Fortov, V. E., & Dianov, E. M. (2006, May). Optical discharge in silica-based fibers: high-speed propagation under kW-range laser radiation. In *Reliability of Optical Fiber Components, Devices, Systems, and Networks III* (Vol. 6193, pp. 241-246). SPIE.

Gega, E., Mitrushi, F., Shano, J., & Firanj, R. (2024). The study of dynamics and quazi zero stiffnes vibration isolator withn numerical integration method. *Buletins of Natural Science.*

Girodano, N. & Nakanishi, H. (2005). *Computational physic using Matlab*. 525 Northwestern Aveue: Prentice Hall.

Goldston, R. & Ratherford, P. (2000). *Introduction to plasma physic*. London.

Hafeez, H. Y., & Ndikilar, C. E. (2014). Van der Pol equation for nonlinear plasma oscillations. *Journal of Advanced Physics*, *3*(4), 278-281.

Keen, B. E., & Fletcher, W. H. W. (1970). Measurement of growth rate, non-linear saturation coefficients, and mode-mode coupling coefficients of a `Van der Pol' plasma instability. *Journal of Physics D: Applied Physics*, *3*(12), 1868.

Lankin, A. V., & Norman, G. E. (2009). Collisional recombination in strongly coupled plasmas. *Journal of Physics A: Mathematical and Theoretical*, *42*(21), 214042.

Maiorov, S. A., Tkachev, A. N., & Yakovlenko, S. I. (1991). Investigation of the fundamental properties of a Coulombian plasma by the method of many-particle dynamics. *Soviet Physics Journal*, *34*(11), 951-976.

Maria de Fátima, F. D., de Brito Paixão, T., Mesquita, E. F. T., Alberto, N., Frias, A. R., Ferreira, R. A., ... & de Brito Andre, P. S. (2015). Liquid hydrostatic pressure optical sensor based on micro-cavity produced by the catastrophic fuse effect. *IEEE Sensors Journal*, *15*(10), 5654-5658.

McGreivy, N. (2017). General Plasma Physics I Notes.

Miwadinou, C. H., Hinvi, L. A., Monwanou, A. V., & Chabi Orou, J. B. (2013). Nonlinear dynamics of plasma oscillations modeled by a forced modified Van der Pol-Duffing oscillator. *arXiv preprint arXiv:1308.6132*.

Rao, Y. J., Ran, Z. L., & Gong, Y. (2017). *Fiber-Optic Fabry–Perot Sensors*. Boca Raton.

Semenov, I. B., Mitrishkin, Y. V., Subbotin, A. A., Vertinskiĭ, A. G., Marusov, N. L., & Sushin, I. S. (2006). A van der pol coupled-oscillator model as a basis for developing a system for suppressing MHD instabilities in a tokamak. *Plasma Physics Reports*, *32*, 114-118.

Shuto, Y. (2018). Cavity generation modeling of fiber fuse in single-mode optical fibers. In P. Steglich & F. De Matteis (Eds.), *Fiber Optics - From Fundamentals to Industrial Applications*. IntechOpen.

Shuto, Y. (2020). Cavity pattern formation and its dynamics of fiber fuse in single-mode optical fibers. *Journal of Informatics and Mathematical Sciences*, *12*(4), 271-288.

Shuto, Y. (2021). Fiber Fuse Phenomenon.

Smirnov, B. M. (2001). Fundamentals of Ionized Gases.

Strogatz, S. H. (2003). *Nonlinear Dynamics and Chaos*. Bristol and Philadelphia: Institute of Physics Publishing.

Van der Pol, B. (1926). On "relaxation-oscillations". *The London, Edinburgh, and Dublin Philosophical Magazine and Journal of Science*, *2*(11), 978-992.

Yakovlenko, S. I. (2006, April). Plasma in bright spot and nature of void chain in fiber fuse track. In *International Conference on Lasers, Applications, and Technologies 2005: Laser-Assisted Micro-and Nanotechnologies* (Vol. 6161, pp. 160-165). SPIE.

Yakovlenko, S. I. (2006). Mechanism for the void formation in the bright spot of a fiber fuse. *Laser Physics*, *16*, 474-476.